


ENERGETIC ASPECTS OF THE DEVELOPMENT OF CONILON COFFEE IN THE NORTH OF RIO DE JANEIRO. PART 1 - RADIATION BALANCE

 <https://doi.org/10.56238/arev6n3-304>

Submitted on: 22/10/2024

Publication date: 22/11/2024

José Carlos Mendonça¹, Mateus Peixoto Pires², Elias Fernandes de Sousa³, Jean Karlos Barros Galote⁴, Thieres George Freire da Silva⁵, Dhiego da Silva Sales⁶ and Daniela Barros de Oliveira⁷

ABSTRACT

Conilon coffee represents a good portion of Brazilian coffee growing and it is essential to understand how the crop relates to the energy available in the environment. Due to this, this work sought to determine the components of the radiation balance of the Conilon coffee crop in the North Fluminense region during seven seasons. The experiment was conducted in a crop field in the area belonging to the Universidade Estadual do Norte Fluminense Darcy Ribeiro, in Campos dos Goytacazes, RJ, which contains a micrometeorological station that monitored environmental data between June 2015 and May 2022. With this information, the radiation balance was carried out. Yield data were obtained by the product of the fresh fruit mass and the mass breakdown of the processed product. Global radiation (R_g), which varies according to the season, was the main component of longwave balance (BOL), the factor with the greatest influence on the variation of net radiation (R_n), since BOL presented low intensities and variations. On average, the albedo over the stand was 12% and the fraction of R_g converted into R_n was 64%. It was concluded that the region is climatically suitable for the crop and that the average production was produced 0.08 g of coffee per MJ of net energy.

Keywords: Coffea Canephora. Shortwave Radiation. Radiation Balance Heat Flux.

¹ Dr. in Plant Production, Associate Professor, Laboratory of Agricultural Engineering - Leag, State University of Norte Fluminense Darcy Ribeiro - UENF, Campos dos Goytacazes, RJ

E-mail: mendonca@uenf.br

² Master in Plant Production, Laboratory of Agricultural Engineering - Leag, State University of Norte Fluminense Darcy Ribeiro – UENF

E-mail: meteuspeixo1@gmail.com

³ Dr. in Plant Production, Full Professor, Laboratory of Agricultural Engineering - Leag, State University of Norte Fluminense Darcy Ribeiro - UENF

E-mail: efs@uenf.br

⁴ Dr. in Plant Production, Laboratory of Agricultural Engineering - Leag, State University of Norte Fluminense Darcy Ribeiro – UENF

E-mail: jean-karlos10@hotmail.com

⁵ Dr. in Meteorology, Associate Professor at the Federal Rural University of Pernambuco – UFRPE, Serra Talhada, PE

Email: thieres.silva@ufrpe.br

⁶ Master in Environmental Engineering. Fluminense Federal Institute, Campos dos Goytacazes, RJ

E-mail: dhiego.sales@outlook.com

⁷ Dr. in Sciences, Associate Professor, Food Technology Laboratory – LTA, Universidade Estadual do Norte Fluminense Darcy Ribeiro - UENF, Campos dos Goytacazes, RJ

E-mail: dbarrosoliveira@uenf.br

INTRODUCTION

The study of the interaction of coffee plantations with solar radiation is of paramount importance for a better understanding and conduction of crops, since it is this that provides energy for the photosynthetic process, and also modulates several other plant physiological processes. In addition, in addition to being an energy source for plants, solar energy also affects other climatic variables such as air and soil temperature, relative humidity, and rainfall, which in turn directly impact plant productivity (Mares et al., 2021). With the use of radiation balance, it is possible to calculate solar energy flow in the productive environment, through shortwave balance (BOC) in addition to longwave balance (BOL) (Querino et al., 2022). The energy balance is based on the principle of conservation of energy, which in this case enters the system in the form of radiation. Partitioning this allows quantifying carbon assimilation, canopy temperature, and the need for water for the crop as a function of the stages of its development, among other parameters (Veloso et al., 2020; Acharya and Sharma, 2021). In Brazil and around the world, there are academic studies that involve the study of atmospheric variables and the physiological behavior of coffee trees (Costa et al., 2019; Angelo et al., 2019; Holwerda and Meesters, 2019). Some studies consider in their studies the radiation balance of coffee intercropped with other crops such as banana (Pezzopane et al., 2005), macadamia nut (Pezzopane et al., 2010), rubber tree (Araújo et al., 2016), *Erythrina poeppigiana* (Vezy et al., 2018), among others. The objective of this study was to determine the radiation balance on the Conilon coffee crop from data from a micrometeorological station in the North Fluminense Region.

Global solar radiation is an extremely important meteorological element, as it provides energy for the vaporization of water (Gentil, 2010). Solar irradiance is the main source of energy for the entire biosphere (Pinto et al., 2022), and plants have the ability to convert electromagnetic energy, coming from the sun, into chemical energy in the form of carbohydrates.

The Sun provides most of the energy used in evapotranspiration, and because of this, the net radiation balance (R_n) is one of the main meteorological elements in the control of evapotranspiration (Rosenberg et al., 1983; Pinto et al., 2022).

This balance is the net energy available for the physical processes of water vaporization to occur both inside the stomata (transpiration) and on the surfaces of the soil and the plant (evaporation). The radiation balance is performed by adding the Shortwave Balance and the Long Wave Balance (Querino et al., 2022).

Querino et al. (2017) cite that the Shortwave Balance is given by the difference between Global Solar Radiation, which is the fraction of Extraterrestrial Solar Radiation that reaches the surface and Reflected Solar Radiation, and that the latter is a function of the albedo of the surface that is receiving solar irradiation.

The surface albedo varies as a function of the roughness, color, and moisture level of the surface, and the darker, rougher, and wetter the surface, such as a forest environment, the lower its value and then the more energy will be available to that ecosystem (Fernandes et al., 2021). In addition, this albedo is also influenced by solar tilt and cloudiness (André et al., 2010a; Schöffel et al., 2021).

Short waves are considered to be those with a length between 30 nm and 300 nm (Bergamaschi and Bergonci, 2017). According to Cui et al. (2012), this type of radiation is fundamental for studies regarding photosynthesis, air and soil heating, evaporation and evapotranspiration.

The Long Wave Balance, on the other hand, is the contribution of atmospheric radiation, where suspended particles emit radiation proportional to their temperature and emissivity (Krieger et al., 2020). Long waves are considered to be those with a length above 300 nm (Bergamaschi and Bergonci, 2017).

As the surface of crops also emits long waves, the balance is made by the difference between the waves received by the atmosphere and emitted by the plant, in the case of agrometeorological studies. Thus, the behavior of long waves depends on atmospheric gases, surface air temperature, and is fundamental in understanding heat exchange (Aguilar et al., 2015).

MATERIALS AND METHODS

The experiment was carried out in an existing crop field in an area belonging to the evapotranspirometric station of the State University of Norte Fluminense Darcy Ribeiro - UENF, located on the premises of the State Center for Research in Agroenergy and Waste Use - CEPEAA, of the Agricultural Research Company of the State of Rio de Janeiro PESAGRO-RIO, in Campos dos Goytacazes, RJ, Brazil, at geographic coordinates 21° 24' 48" South latitude and 41° 44' 48" West longitude and 14 m altitude, referring to Datum WGS84.

According to the Köppen climate classification, the climate of the region is classified as Aw, that is, a humid tropical climate, with a rainy summer, a dry winter and an average

air temperature in the coldest month above 18°C. According to the last climatological normal of the municipality (1991-2020), the average temperature is around 24.6°C, with an average annual rainfall of 981.6 mm, the presence of dry spells in the months of January and February is common (INMET, 2023).

Data on incident solar radiation, net radiation, maximum and minimum temperature and relative humidity, rainfall, wind speed and direction, among others, were obtained by means of a micrometeorological station installed on the coffee tree canopy.

The soil of the experimental area has a flat topography and is classified as Dystrophic Tb Fluvic Neosol, according to the Brazilian soil classification system of EMBRAPA (1999).

The spacing used between the coffee trees is 2.5 m between rows and 1.5 m between plants in the row, totaling an area of 22.5 m² per subplot and useful area of the subplot with 15 m². Each subplot consists of six plants, and the two ends are considered borders (Figure 1). The total experimental area was 1260 m².

The genotypes used are clones of the Vitória variety: clone 02 with early cycle, and the pollinating clones were: clone 3V (medium cycle), clone 6V (medium cycle), clone 11V (early cycle) and clone P2 (medium cycle). The use of different genetic materials in the same area is due to *C. canephora*'s characteristic of cross-fertilization (Venancio et al., 2020).

Figure 1: Aerial view of the arrangement of plants and spacing in the experimental area, Campos dos Goytacazes, RJ. Source: Prof. José Carlos Mendonça.



The plants were transplanted to the site in May 2014, and the evaluations described in the present study were carried out from June 1, 2015 to May 31, 2022. The production cycle was considered from the beginning of June of one year to the end of May of the following year.

At the beginning of the cultivation, liming was determined by the Base Saturation Method and sought to reach the value of 70%, and for this purpose a superficial application of dolomitic limestone was used 90 days before transplanting. Fertilization was carried out in holes, with the incorporation of 200 g of simple superphosphate, 5.0 L of barnyard manure and 20 g of barnyard manure formulated with micronutrients FTE – BR 12, which contains 1.8% of B, 0.8% of Cu, 2.0% of Mn, 9.0% of Zn and 1.0% of S, according to the recommendation for culture (Garcia et al., 2022; Prezotti, 2014).

The cultural and phytosanitary treatments were carried out according to the technical recommendations of the crop. (Ferrão, et al., 2017). The coffee plantation was harvested around May of each year and afterwards, the skeletonization of the plants was carried out, in order to prepare them for the next production cycle.

The crop was irrigated by drip, and the irrigation depths were calculated based on the ETo, calculated by the Penman-Monteith method (Allen et al., 1998) based on data from a meteorological station near the crop area.

In the experimental area, a micrometeorological station was installed to measure global solar radiation and reflected solar radiation, radiation balance, temperature and relative humidity, wind speed and direction, and heat flux on the ground.

For the measurements of global solar radiation (Rg) and reflected radiation (Rr) by the surface, two LI-200X Li-Cor pyranometers were used, Lincoln, NE, USA, one with the face facing up and the other with the face facing down. The radiation balance (Rn) was obtained by a balance radiometer model NR-Lite Kipp and Zonen Campbell Scientific Inc., Logan, Utah, USA. The pyranometers and the balance radiometer were positioned 0.5 m above the coffee canopy.

Temperature and relative humidity data were obtained using HMP45C-L probes, Vaisala, Helsinki, Finland, while wind speed and direction were measured by two Met One 03002 shell anemometers - L R. M. Young Wind Sentry Set, Campbell Scientific Inc., Logan, Utah, USA. Both the probes and the anemometers were installed 0.5 m and 2.5 m above the canopy, so that it was possible to obtain a gradient of temperature, air humidity and wind speed. Three flowmeters model HFP01SC-L Hux Flux Thermal Sensors, Campbell Scientific Inc., Logan, Utah, USA, at 0.02 m depth, were also used to account for the heat flux in the soil (G).

Data were collected every minute and stored at average values every 15 minutes by a CR1000 data collector from Campbell Scientific Inc., Logan, Utah, USA.

By means of the ratio between the reflected solar irradiance and the hourly average incident it is possible to obtain the albedo, which was calculated by Equation 1:

$$\alpha = \frac{Rr}{Rg} \quad \text{Eq. 1}$$

Where:

α is the albedo, dimensionless;

Rr is reflected solar radiation, MJ.m⁻².day⁻¹;

Rg is the incident solar radiation, MJ.m⁻².day⁻¹.

For the daily albedo, only the mean albedos between 11 a.m. and 1 p.m. were considered, as done by André et al. (2010a), when the sun's rays are falling at a lower zenith angle.

The angular coefficients (a) and linear coefficients (b) of the regression between the radiation balance (Rn) and the difference between Rg and Rr were also calculated, according to André et al. (2010a). From the regression coefficients, the long-wave exchange coefficient (λ_L), a parameter referring to the thermal properties of the air, was calculated using Equation 2:

$$\lambda_L = a - 1 \quad \text{Eq. 2}$$

Where:

λ_L is the long-wave, dimensionless exchange coefficient;
a is the slope of the regression between Rn and (Rg-Rr).

Also from the regression reported above, the thermal coefficient (β_L), a parameter related to the thermal properties of the surface, was calculated using Equation 3:

$$\beta_L = \frac{1 - a}{a} \quad \text{Eq. 3}$$

Where:

β_L is the thermal coefficient, dimensionless;
a is the slope of the regression between Rn and (Rg-Rr).

Atmospheric transmissivity (Kt) indicates how much particles in the atmosphere influence the solar radiation that reaches the surface and was calculated by Equation 4, according to André et al. (2010a):

$$Kt = \frac{Rg}{R_a} \quad \text{Eq. 4}$$

Where:

Kt is atmospheric transmissivity;
Rg is the incident solar radiation, in MJ.m⁻².day⁻¹;

Ra is solar radiation at the top of the atmosphere, MJ.m⁻².day⁻¹.

Kt<0.4 indicates a day with high cloudiness; 0.4≤Kt<0.6, represents a day with partly cloudy skies, while Kt≥0.6 demonstrates clear skies and low cloudiness conditions (Querino et al., 2022).

The solar radiation at the top of the atmosphere was calculated by Equation 5 described by Alves and Vianello (2004):

$$Ra = S_0 \left(\frac{D'}{D} \right)^2 \cos Z \quad \text{Eq. 5}$$

Where:

Ra is solar radiation at the top of the atmosphere, MJ.m⁻².day⁻¹;

S0 is solar constant, in MJ.m⁻².day⁻¹;

D' is the earth-sun distance;

D'/D is the correction factor due to the eccentricity of the earth's orbit;

Z is the zenith angle, in °.

The shortwave balance was calculated based on equation 6:

$$BOC = Rg (1 - \alpha) \quad \text{Eq. 6}$$

To obtain the longwave balance, the difference between the radiation balance and the shortwave balance was calculated, as André et al. (2010a), as shown in equation 7:

$$BOL = Rn - BOC \quad \text{Eq. 7}$$

Where:

ΔL is the longwave balance, in MJ m⁻².day⁻¹;

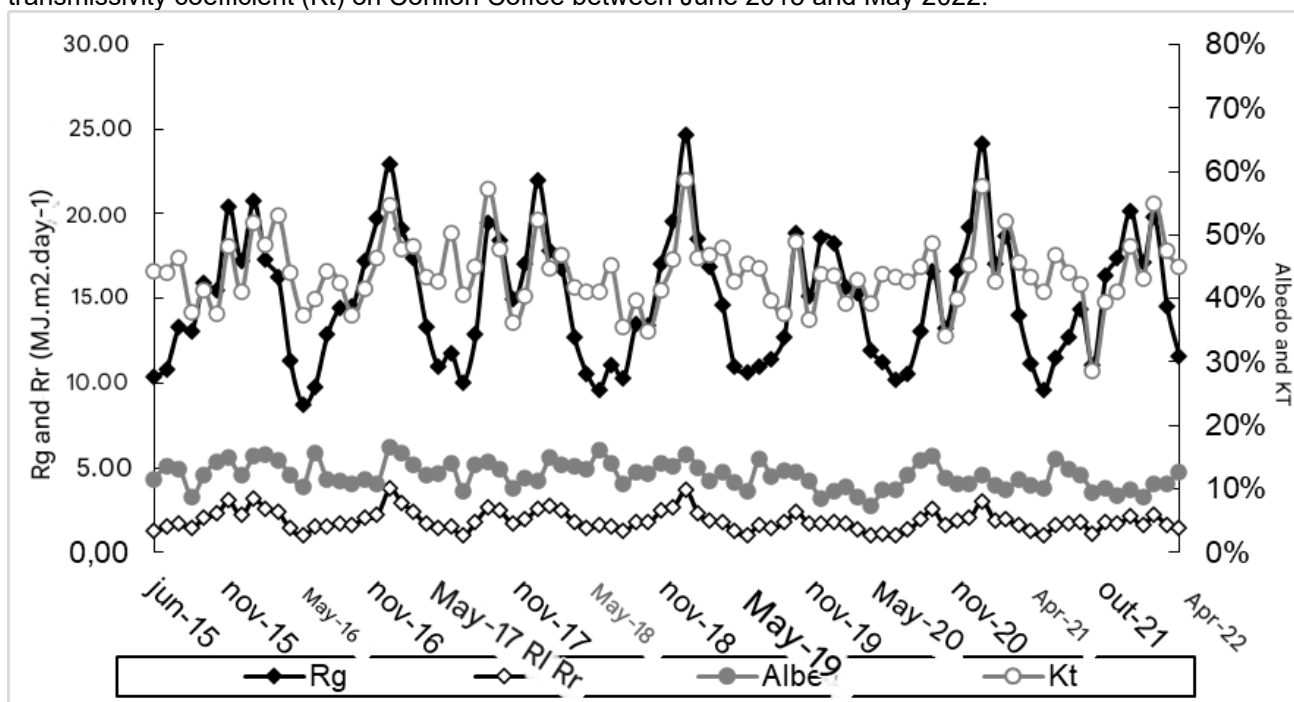
α is the albedo of the surface;

Rg is the global solar radiation, in MJ m⁻².day⁻¹.

RESULTS AND DISCUSSION

Solar radiation is the main source of energy for the biosphere and due to this it is essential to understand how this climate variable behaves (Pinto et al., 2022). For this, Figure 4 presents the monthly averages of global solar radiation (Rg), reflected solar radiation (Rr), as well as albedo and transmissivity coefficient (Kt) in the experimental area from June 2015 to May 2022.

Figure 2: Monthly averages of global solar radiation (Rg), reflected solar radiation (Rr), albedo and transmissivity coefficient (Kt) on Conilon Coffee between June 2015 and May 2022.



By observing Figure 2, it is possible to notice that global solar radiation presents higher values in the first months of the year, reduces its intensity as the months go by, until it presents its minimums in the middle months and then starts to intensify until it reaches its maximum values in the following year, as well as the temperature. This similarity in patterns is due to solar radiation exerting a strong influence on air temperature (Azeez, 2022). Radiation variation, on the other hand, is explained by latitude and astronomical factors (solar declination and terrestrial translation), in addition to atmospheric composition (Querino et al., 2022).

The maximum value of Rg observed was 24.64 MJ.m⁻².day⁻¹, in January 2019, which indicates a high atmospheric demand for humidity. Other peaks of monthly solar radiation can also be observed in December 2016 and January 2021 (22.92 MJ.m⁻².day⁻¹

and 24.19 MJ.m⁻².day⁻¹, respectively), which can be explained by the slightly higher cloudiness, indicated by a lower transmissivity coefficient.

It can be observed that in the transition from 2015 to 2016, from 2017 to 2018, from 2019 to 2020 and from 2021 to 2022 there was an oscillation in the behavior of the incidence of solar radiation, which meant that it did not reach higher peaks. This fact is also explained by atmospheric transmissivity and rainfall in the region, common for the season, as it is the rainy season in the region (Mendonça et al., 2021).

The minimum value of R_g obtained during the experiment was 8.71 MJ.m⁻².day⁻¹, in June 2016 due to a lower incidence of extraterrestrial solar radiation, due to astronomical factors, combined with a K_t of 37%, below the average of the months of June (43%). Usually the lowest values of R_g are observed in June, except in 2017, which had July, the month of lower solar incidence.

The transmissivity coefficient represents the influence of the atmosphere on the solar radiation incident on the surface, through particles suspended in the air, which increase its atmospheric opacity (Querino et al., 2022). Thus, it can be used to measure cloudiness, as done by André et al. (2010a). During the experimental period, the average K_t was 44%, a condition classified as partly cloudy (40% > K_t > 60%).

Not even the month with the highest average K_t, January 2019, was classified as clear skies (K_t > 60%), reaching only 59%. On the other hand, the lowest K_t observed was 29%, in October 2021, and was classified as cloudy, as were 17 of the 84 months evaluated. It can also be noted that K_t varies in a similar way to R_g, especially in the months of higher solar incidence, while in the months of lower global radiation, although these variables continue in phase, the intensity of the relationship decreases. This fact occurs as a result of extraterrestrial solar radiation (R₀) becoming more limiting in these periods.

When observing the reflected solar radiation (Figure 2), it is noted that the maximum value obtained was 3.76 MJ.m⁻².day⁻¹, in January 2017, while the minimum was 0.99 MJ.m⁻².day⁻¹, in July of the same year. Although the months of which the maximum values did not coincide, as well as the months of minimums, it is possible to observe that R_g and R_r have similar behavior, since the reflected radiation depends on the incident.

However, the surface also has a great influence on the reflection of radiation, and to measure this action, the albedo is used, which is the R_r/R_g ratio. Even though it is the main factor, the albedo does not depend only on the characteristics of the surface, but also on

the inclination of the incidence of rays, as well as on the proportion of direct and diffuse radiation that reaches a given surface (Ataide et al., 2020).

The average albedo on coffee cultivation in the period evaluated was 12.16%, within the normal range observed in agricultural crops, whose averages range from 11% to 26% (Banerjee and Dutta, 2016; Ferreira et al., 2020; Bakanoğullari et al., 2022).

In the experimental area, the albedo is influenced by the water status of the Conilon, its physiological cycles (vegetative and reproductive cycle) and by the cultural treatments applied to it. These elements can influence the leaf area of the crop and the color of the leaves, characteristics that interfere in the dynamics of solar radiation reflection.

The highest albedo value was 16.59%, obtained in January 2017, when the plants were in granation (filling) of the fruits, a phase in which a large increase in dry matter in the grains (Ferrão et al., 2017).

The high value observed is due to the water deficit to which the crop was subjected, given that despite a considerable volume of rain in January 2017 and in the previous months, there were 17 days without water entering the crop between the end of 2016 and the beginning of 2017, either by irrigation, or by precipitation. This set of factors caused loss of leaf vigor and yellowing, and also, drier surfaces tend to be lighter in color than humid ones, which increases the reflection of solar radiation from them (Querino et al., 2006).

The lowest albedo was 7.32% in April 2020, when there was an accumulated of 455.3 mm in the last three months, in addition to an accumulated of 87.6 mm during the month of April itself, which indicates high water availability for cultivation. In addition, the fruits were going through the maturation phase and the plants were at their maximum size, before going through the leaf senescence at the end of the maturation period and the skeleton pruning carried out post-harvest.

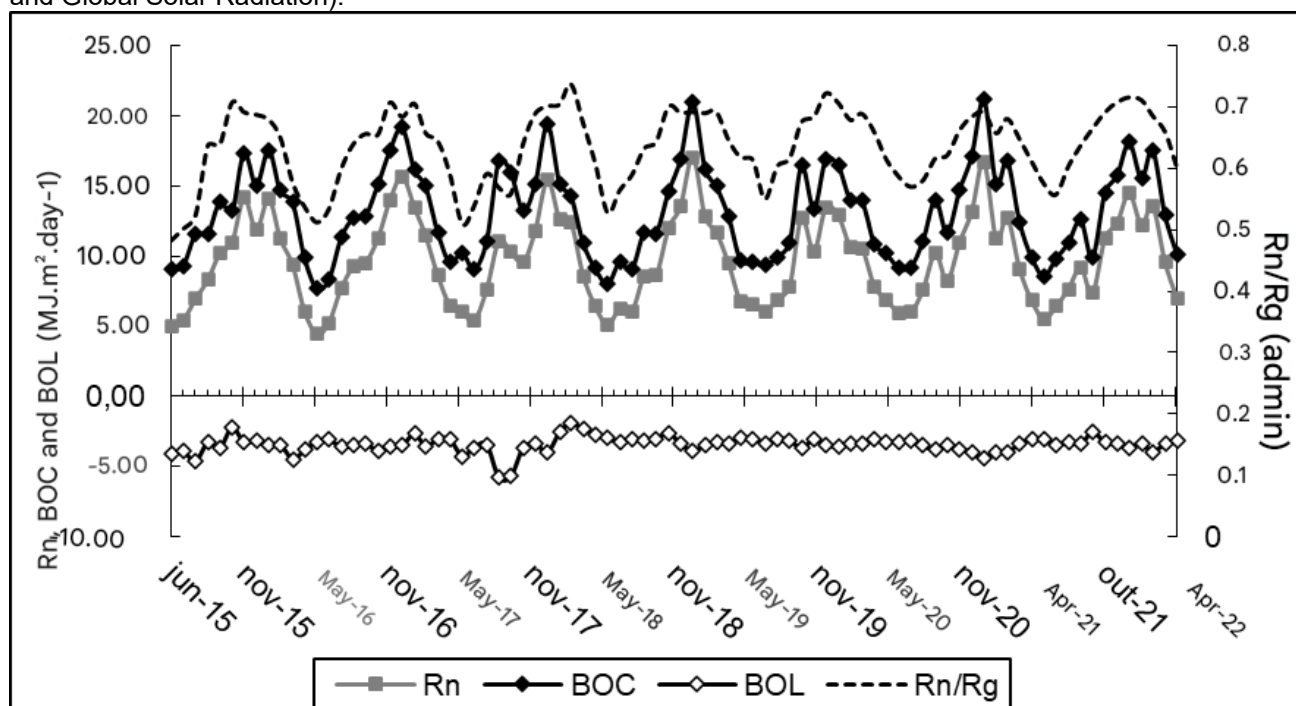
Thus, the cultivation was vigorous, with a larger leaf area and dark green leaves, characteristics that contribute to greater trapping of sunlight, which decreases albedo (Yuan et al., 2022).

In general, it can be seen that large increases in albedo values occur during periods of stress in plants, or shortly after them. Normally, the acute increases in albedo in the hottest period of the year are due to water stress caused by small summers, supplementation by irrigation, while in the coldest season it was also caused by water

stress. Lower albedo values imply a higher balance of shortwave radiation, increasing the net energy available for water heating and evaporation processes.

For a better understanding of the behavior of radiant energy availability for cultivation, Figure 3 presents the monthly averages of net radiation (Rn), shortwave balance (BOC), longwave balance (BOL) and the Rn/Rg ratio.

Figure 3: Monthly Radiation Balance over Conilon Coffee between June 2015 and May 2022. (Rn – Net radiation; BOC - Short Wave Swing; BOL – Long Wave Swing; Rn/Rg – Ratio between the Radiation Balance and Global Solar Radiation).



When looking at Figure 3, it can be seen that the BOC varies mainly due to the Rg, since the Rr values have low intensity values, a fact also observed by Querino et al. (2022). Thus, the BOC have higher values in the first months of the year, tend to decrease until June or July, when they start to increase again.

The average shortwave balance value observed was 13.11 MJ.m⁻².day⁻¹, with a maximum of 21.15 MJ.m⁻².day⁻¹, in January 2021. On the other hand, the lowest BOC value was 7.67 MJ.m⁻².day⁻¹, obtained in June 2016, a month in which the Rg was also minimal.

The longwave balance, in turn, is the difference between the infrared radiation emitted by the atmosphere (Ra), which varies as a function of the atmospheric composition and air temperature, and the infrared radiation emitted by the surface (Rs), which depends

on the temperature and emissivity of the surface (Querino et al., 2020; Querino et al., 2022).

The BOL presented negative monthly values throughout the experiment, which indicates that it contributed to the energy output of the productive environment. The mean BOL value observed was $-3.42 \text{ MJ.m}^{-2}\text{.day}^{-1}$. The maximum value of BOL was $-1.89 \text{ MJ.m}^{-2}\text{.day}^{-1}$, in March 2018, which can be explained by the high value of R_a , which counts positively in the balance, which makes the value less negative.

In that month, RH was above the average for the month of March (3.46% higher), in addition to presenting the highest monthly accumulation of rainfall (271 mm), however, the air temperature showed values very close to the average of the period (26.54°C). High air temperatures, greater amounts of water vapor in the atmosphere, fog, and precipitation are directly related to the increase in R_a (Nyeki et al., 2019; Pinto et al., 2022; Querino et al., 2022).

On the other hand, the minimum BOL value of $-5.73 \text{ MJ.m}^{-2}\text{.day}^{-1}$, in September 2017, the month in which there was more energy output from the cultivation environment by long waves. In this month, low cloudiness (Kt of 57%) and RH (71.07%) were observed, which indicates low emission of long waves from the atmosphere, in addition to a high value of R_g ($19.46 \text{ MJ.m}^{-2}\text{.day}^{-1}$), which causes the soil and plant surfaces to receive more energy and emit more longwave radiation (R_s).

It can be observed that BOL does not present a well-defined pattern of annual variation, since several factors interfere, while the BOC has a very variable function of R_g and Kt. In addition, it is possible to note that the amplitude and absolute value of BOL are much lower than those of the BOC.

Also according to Figure 3, the average value of net radiation observed during the experiment was $9.69 \text{ MJ.m}^{-2}\text{.day}^{-1}$, with a maximum of $17.05 \text{ MJ.m}^{-2}\text{.day}^{-1}$, in January 2019, when the R_g was also a maximum and a minimum of $4.46 \text{ MJ.m}^{-2}\text{.day}^{-1}$, in June 2016, together with the minimum R_g .

As previously mentioned, the maximum and minimum values observed are due to atmospheric transmissivity and astronomical factors, which impact the BOC, which represents the most influential factor in R_n . Veloso et al. (2020) also observed that in the summer higher values of R_n in the summer and lower in the winter and attributed this fact to global solar radiation. Fernandes et al. (2021) report that in addition to R_g , vegetation is also a factor that influences R_n , as they modify the albedo and decrease the surface

temperature, reducing long-wave emissions, which results in greater energy availability for the productive environment.

For a better understanding of how much of the incident energy was available, Figure 5 also shows the R_n/R_g ratio. The average value of this ratio during the experiment was 0.64, that is, 64% of the incident solar energy is available to the surface, a proportion very close to that obtained by Querino et al. (2022), in the semi-arid region of Alagoas.

This proximity between the result obtained by these authors and that observed in the present work is due to the climatic similarities, since the region of Campos dos Goytacazes is classified according to the Thornthwait climatic classification as dry sub-humid, a classification close to the semi-arid, and the North Fluminense region is going through a process of growth of aridity indicators (Mendonça, 2023).

During the experiment period, the maximum value of R_n/R_g was 0.74, obtained in March 2018, which can be explained by the lower energy output of the productive medium through long waves. On the other hand, the lowest R_n/R_g ratio was 0.48 in June 2015, when the BOL value was below the average during the experiment ($-4.07 \text{ MJ.m}^{-2}.\text{day}^{-1}$) and much lower than in June, the months with the lowest global solar radiation.

The lowest proportion obtained in this month is due to the emission of long waves above average in a month of low incidence of solar radiation. Thus, it can be noted that, due to the low variation in albedo, the factor that most alters the R_n/R_g ratio is the longwave balance. In general, during the hotter and rainier months, the R_n/R_g ratio is higher when compared to the colder and drier months, as observed by Querino et al. (2022).

By the angular coefficient of the regression between the shortwave balance (BOC) and the radiation balance (R_n) it is possible to calculate the thermal coefficient (β_L) and the longwave transformation coefficient (λ_L). In this study, both coefficients were calculated monthly and are shown in Figure 4, together with the values of the coefficient of determination (R^2) of the regression between BOC and R_n .

Figure 4: Thermal coefficient (β_L), longwave transformation coefficient (λ_L) and Coefficient of determination (R^2) of the regression between BOC and Rn in Conilon Coffee between June 2015 and May 2022.

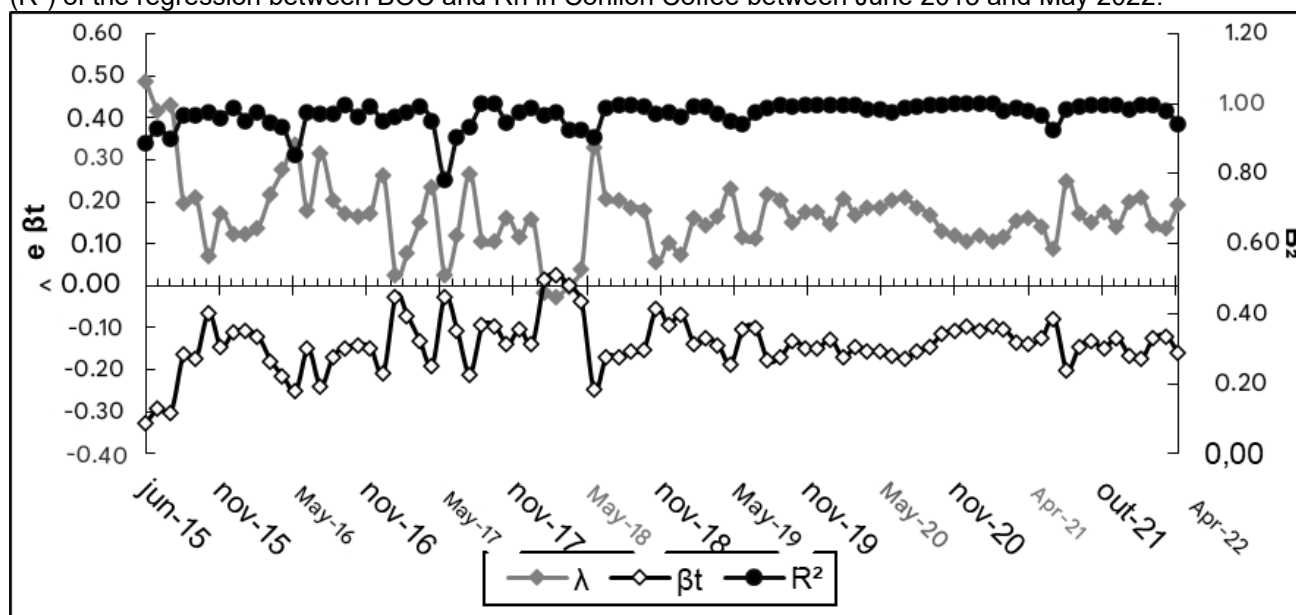


Figure 4 shows that the coefficient of determination (R^2) of the regressions that generated the other coefficients has always remained high, with a mean value of 0.97, which indicates an excellent adjustment. The month that presented the lowest value was June 2017, which had an R^2 of 0.78, which may have been due to the BOC above the average for the month, while the Rn was lower than the average for the months of June. This variation was due to the absence of water entering the productive environment for 10 days in that month, which generated water stress in the coffee plantation.

The λ_L is related to the thermal properties of the air, while the β_L is related to the thermal properties of the surface and indicates the portion of the radiation balance that is converted into long waves (André et al., 2010a), that is, λ_L is related to R_a and β_L , to R_s . According to Azevedo et al. (2014) the increase in leaf area is accompanied by a decrease in β_L and an increase in λ_L , which indicates that the largest portion of the radiation balance is being converted into latent heat.

In general, it can be observed that λ_L and β_L have opposite behaviors, almost symmetrical in relation to the axis of the abscissas, however λ_L has a greater amplitude than β_L . During the study period, λ_L ranged from -0.03 to 0.49, with a mean of 0.17, while β_L ranged from -0.33 to 0.03, with a mean of -0.14.

The only period that β_L was greater than λ_L was from February to April 2018, which indicates that the emission of long waves was higher than the conversion into latent heat. In this period, higher values of BOL were observed (Figure 5), including the highest value

obtained in the entire period ($-1.89 \text{ MJ.m}^{-2}.\text{day}^{-1}$). In Figure 6 it is also possible to see a greater variation at the beginning of the evaluated period, tending to have milder variations over time, which may be due to the better establishment and greater physiological maturity of the coffee trees, in addition, in the 2017/2018 agricultural year, there was water scarcity in the experiment due to technical problems in the irrigation equipment, which may have affected the parameters evaluated.

CONCLUSIONS

Global radiation (R_g), which varies according to the season, was the main component of longwave balance (BOL), the factor with the greatest influence on the variation of net radiation (R_n), since BOL presented low intensities and variations. On average, the albedo over the stand was 12% and the fraction of R_g converted into R_n was 64%. The BOL presented values of quantities much lower than BOC, in addition to not varying with a seasonality as well established as the latter. In addition, the influence of ENSO phenomena on local environmental conditions was observed. In view of the results, it was also concluded that the municipality of Campos dos Goytacazes is suitable for the cultivation of Conilon coffee, as long as it is managed correctly.

REFERENCES

1. Acharya, B., & Sharma, V. (2021). Comparison of satellite-driven surface energy balance models in estimating crop evapotranspiration in semi-arid to arid inter-mountain region. **Remote Sensing, 13*(9), 1822.*
2. Allen, R. G., Pereira, L. S., Raes, D., & Smith, M. (1998). **FAO Irrigation and drainage paper n°. 56.** Rome: Food and Agriculture Organization of the United Nations, 301p.
3. Alves, A. R., & Vianello, R. L. (2004). **Meteorologia básica e aplicações.** Viçosa: Editora da UFV.
4. André, R. G. B., Mendonça, J. C., Marques, V. D. S., Pinheiro, F. M. A., & Marques, J. (2010). Aspectos energéticos do desenvolvimento da cana-de-açúcar. Parte 1: balanço de radiação e parâmetros derivados. **Revista Brasileira de Meteorologia, 25*, 375-382.*
5. Angelo, P. C. S., Ferreira, I. B., de Carvalho, C. H. S., Matiello, J. B., & Sera, G. H. (2019). Arabica coffee fruits phenology assessed through degree days, precipitation, and solar radiation exposure on a daily basis. **International Journal of Biometeorology, 63*, 831-843.*
6. Aguilar, J. L. C., Gentle, A. R., Smith, G. B., & Chen, D. (2015). A method to measure total atmospheric long-wave down-welling radiation using a low-cost infrared thermometer tilted to the vertical. **Energy, 81*, 233-244.*
7. Araújo, A. V., Partelli, F. L., Oliosi, G., & Pezzopane, J. R. M. (2016). Microclimate, development and productivity of robusta coffee shaded by rubber trees and at full sun. **Revista Ciência Agronômica, 47*, 700-709.*
8. Ataíde, W. L. da S., de Oliveira, F. D. A., & Pinto, C. A. D. (2020). Balanço de radiação, energia e fechamento do balanço em uma floresta prístina na Amazônia oriental. **Revista Brasileira de Geografia Física, 13*(06), 2603-2627.*
9. Azeez, L. (2022). Demonstration of net solar radiation geographical behavior reverse correlation with relative humidity in Iraq. **Iraqi Journal of Science, 63*(6), 2741–2754.* <https://doi.org/10.24996/ijcs.2022.63.6.38>
10. Azevedo, P. V. D., Saboya, L. M., Dantas Neto, J., Oliveira, F. D. S., Bezerra, J. R., & Farias, C. H. D. A. (2014). Disponibilidade energética para a cultura da cana-de-açúcar nos tabuleiros costeiros do estado da Paraíba. **Revista Brasileira de Engenharia Agrícola e Ambiental, 18*, 1031-1038.*
11. Bakanoğullari, F., Şaylan, L., & Yeşilköy, S. (2022). Effects of phenological stages, growth and meteorological factors on the albedo of different crop cultivars. **Italian Journal of Agrometeorology**. <https://doi.org/10.36253/ijam-1445>
12. Banerjee, S., & Dutta, P. (2016). Albedo pattern over rice field in lower Gangetic Plains of West Bengal during Kharif and Boro seasons. **Indian Journal of Applied Research, 5.**

13. Bergamaschi, H., & Bergonci, J. I. (2017). **As plantas e o clima: princípios e aplicações.** Guaíba: Agrolivros.
14. Costa, J. D. O., Coelho, R. D., Barros, T. H. D. S., Fraga, E. F., & Fernandes, A. L. T. (2019). Leaf area index and radiation extinction coefficient of a coffee canopy under variable drip irrigation levels. **Acta Scientiarum. Agronomy, 41.**
15. Cui, Y., Liu, J., Hu, Y., Wang, J., & Kuang, W. (2012). Modeling the radiation balance of different urban underlying surfaces. **Chinese Science Bulletin, 57**, 1046-1054.
16. EMBRAPA - Empresa Brasileira de Pesquisa Agropecuária. (1999). **Sistema Brasileiro de Classificação de Solos.** Rio de Janeiro: Embrapa, 412p.
17. Fernandes, G. S. T., Lopes, P. M. O., de Melo, C. G. B., Lima, R. L. F., dos Santos, A., & de Oliveira Silva, D. A. (2021). Balanço de radiação em áreas de expansão agrícola no Sudoeste do Piauí. **Revista de Geociências do Nordeste, 7*(1), 13-20.*
18. Ferrão, R. G., Fonseca, A. F. A., Ferrão, M. A. G., & Muner, L. H. (2017). **Café Conilon.** 2ª ed. Vitória, ES: Incaper.
19. Ferreira, T., Silva, B., Moura, M., Verhoef, A., & Nóbrega, R. (2020). The use of remote sensing for reliable estimation of net radiation and its components: A case study for contrasting land covers in an agricultural hotspot of the Brazilian semiarid region. **Agricultural and Forest Meteorology**. <https://doi.org/10.1016/j.agrformet.2020.108052>
20. Garcia, A. D. B., Mendonça, J. C., Almeida, C. M., Lazzarini, L. M., & Ribeiro, C. C. (2022). Optimum economic irrigation levels of conilon coffee (**Coffea canephora**) in the North Fluminense Region, Brazil. **Journal of Agricultural Sciences Research, 2*(2).*
21. Gentil, M. S. (2010). **Transpiração e eficiência do uso da água em árvores clonais de Eucalyptus aos 4 anos em áreas com e sem irrigação em Eunápolis, Bahia** (Master's dissertation, Escola Superior de Agricultura "Luiz de Queiroz"). 71 p.
22. Holwerda, F., & Meesters, A. G. C. A. (2019). Soil evaporation in a shaded coffee plantation derived from eddy covariance measurements. **Journal of Geophysical Research: Biogeosciences, 124**, 1472–1490. <https://doi.org/10.1029/2018JG004911>
23. INMET – Instituto Nacional de Meteorologia. (2023). **Normais climatológicas – Período de 1991 – 2020**. Disponível em: <https://portal.inmet.gov.br/normais>. Acesso em 17 de janeiro de 2023.
24. Krieger, J. M., Vieira, I. S., da Silva, W. D. O. A., Souza, J. L., Lyra, G. B., & Lyra, G. B. (2020). Balanço de radiação utilizando métodos de estimativa da radiação solar em cultivo de cana-de-açúcar. **Agrometeoros, 27*(1).*
25. Mares, C., Mares, I., Dobrica, V., & Demetrescu, C. (2021). Quantification of the Direct Solar Impact on Some Components of the Hydro-Climatic System. **Entropy, 23**. <https://doi.org/10.3390/e23060691>

26. Mendonça, J. C. (2023). Índices hídricos, de aridez e de umidade na região norte do estado do Rio de Janeiro. In Guedes, D. M., da Silva, L. F., & de Oliveira, V. C. *Avances científicos y tecnológicos en ciências agrícolas 3* (pp. 8–20). 1ª ed. Ponta Grossa: Atena Editora.
27. Mendonça, J. C., Garcia, A. D. B., & de Almeida, C. M. (2021). Efeito de diferentes lâminas de irrigação na uniformidade de grãos moca do café Conilon, em Campos dos Goytacazes, RJ. *IRRIGA, 26*(2), 411–421.
28. Nyeki, S., Wacker, S., Aebi, C., Gröbner, J., Martucci, G., & Vuilleumier, L. (2019). Trends in surface radiation and cloud radiative effect at four Swiss sites for the 1996–2015 period. *Atmospheric Chemistry and Physics, 19*(20), 13227–13241.
29. Pezzopane, J. R. M., Pedro Júnior, M. J., & Gallo, P. B. (2005). Radiação solar e saldo de radiação em cultivo de café a pleno sol e consorciado com banana 'Prata Anã'. *Bragantia, 64*, 485–497.
30. Pezzopane, J. R. M., Marsetti, M. M. S., Souza, J. M. D., & Pezzopane, J. E. M. (2010). Condições microclimáticas em cultivo de café Conilon a pleno sol e arborizado com noqueira macadâmia. *Ciência Rural, 40*, 1257–1263.
31. Pinto, J. V. D. N., Costa, D. L. P., Nunes, H. G. G. C., Silva Junior, A. C. D., Sousa, A. M. L. D., Souza, P. J. D. O. P. D., & Ortega-Farias, S. (2022). Radiation Balance and Partitioning of Latent and Sensible Heat Fluxes over a Lime Orchard in Eastern Amazon. *Revista Brasileira de Meteorologia, 37*, 491–502.
32. Prezotti, L. C. (2014). *Sistema de recomendação de calagem e adubação*. Disponível em: Acesso em 25/01/2016.
33. Querino, C. A. S., Biudes, M. S., Machado, N. G., Querino, J. K. A. da S., Moura, M. A. L., & Alves, P. V. (2020). Modelling parametrization to estimate atmospheric long wave radiation in the Northern Mato Grosso, Brazil. *Ciência E Natura, 42*, e105. <https://doi.org/10.5902/2179460X41205>
34. Querino, C. A. S., Júnior, J. M. L., & Moura, M. A. L. (2022). Balanço de Radiação no Bioma Caatinga no Semiárido Alagoano. *Revista Brasileira de Geografia Física, 15*(06), 2715–2729.
35. Querino, C. A. S., Muirdes, M. S., Machado, N. G., da Silva Querino, J. K. A., Neto, L. A. S., Silva, M. J. G., ... & Nogueira, J. (2017). Balanço de ondas curtas sobre floresta sazonalmente alagável do Pantanal Mato-Grossense. *Revista Brasileira de Climatologia, 20*.
36. Schöffel, E. R., dos Santos, P. M., da Rosa Maciel, L., & Herter, F. G. (2021). Fluxos de energia radiante em cultivos de amora-preta 'Tupy'. *Revista Caminhos de Geografia, 22*(8), 169–181.

37. Veloso, G. A., da Silva, L. A. P., & Ferreira, M. E. (2020). Análise do balanço de radiação e energia em áreas de veredas no norte de Minas Gerais, bioma Cerrado. *Cerrados, 18*(1), 220–247.
38. Vezy, R., Christina, M., Roupsard, O., Nouvellon, Y., Duursma, R., Medlyn, B., ... & Le Maire, G. (2018). Measuring and modelling energy partitioning in canopies of varying complexity using MAESPA model. *Agricultural and Forest Meteorology, 253*, 203–217.
39. Yuan, S., Wang, Y., Zhang, H., Zhao, J., Guo, X., Xiong, T., Li, H., & Zhao, H. (2022). Blue-Sky Albedo Reduction and Associated Influencing Factors of Stable Land Cover Types in the Middle-High Latitudes of the Northern Hemisphere during 1982–2015. *Remote Sens, 14*, 895. <https://doi.org/10.3390/rs14040895>